Subexcitation electron interactions in rare gases: Production of electronic excited states in helium or neon mixtures with argon, krypton, or xenon

Ronald Cooper* and Myran C. Sauer, Jr.
Chemistry Division, Argonne National Laboratory, Argonne, Illinois 60439
(Received 11 July 1994)

The formation and decay of the "2*p*" electronic excited states of the rare gases neon, argon, krypton, and xenon in a buffer gas of either helium or neon has been studied by pulse radiolysis techniques. The formation rate constants for these states are all greater than $\sim 2\times 10^{-9}$ cm^3 s^{-1}, precluding atom-atom collisional processes and supporting a subexcitation electron mechanism. The rate constants generally show a trend $k_{Xe} > k_{Kr} > k_{Ar} > k_{Ne}$. Quenching rate constants for the deactivation of some of the 2*p* levels are also reported.

PACS number(s): 34.80.Dp

INTRODUCTION

In previous publications [1–3], we have demonstrated that luminescence from pulse radiolyzed gas mixtures can be used to study the excitation of a minor component of a mixture by electrons with energy below the lowest excited level of the major component. These results demonstrated, in a time-resolved, kinetic fashion, the effects of such electrons, which were named *subexcitation electrons* by Platzman [4,5]. (The role of subexcitation electrons in radiation physics and chemistry has recently been summarized [6].) Subsequent theoretical calculations by Naleway *et al.* [7] confirmed that in helium-nitrogen and neon-nitrogen mixtures, a subexcitation mechanism is fully substantiated. Later experiments using aromatic hydrocarbons as fluorescent probes produced similar data to the nitrogen system, but unfortunately, a lack of electron excitation cross-section data for these species precludes any theoretical study.

The main criterion for a mixed gas system to show subexcitation electron effects is that the luminescent probe gas must have electronic energy levels *below* the lowest excited-state energy level of the bulk gas. To aid theoretical calculations of the time dependence of these phenomena, gases whose cross sections for excitation and ionization are reliably known are the most useful. The rare gases themselves are excellent candidates since, apart from helium, they have experimentally observable excited-state emissions (2*p* levels), and they show a convenient stepwise decrease in lowest energy level with increasing atomic number. A considerable amount of reliable cross-section data is available for all these gases.

We have previously shown that analysis of the luminescence data, which gives the relative concentrations of excited states of the minor components as a function of time, yields an effective rate constant for the interaction of the subexcitation electrons with the minor component. It is clear that the subexcitation electrons have a distribution of energies and cannot be rigorously treated as a simple chemical reactant; however, the effective rate constant obtained is a convenient parameter for describing their interactions with the minor component in an irradiated system and is closely related to the excitation cross sections of the subexcitation electrons. It should be pointed out that the pulse radiolysis technique used in such experiments ionizes less than one atom in 10^6 [3×10^{12} ions/cm^3 in $\sim$13 kPa (100 torr) of gas]. This precludes significant energy loss by interactions among the charged particles and changes in the number density by ion recombination. The latter process is seen to occur in these systems on a time scale more than an order of magnitude longer than the subexcitation electron interactions. This study examines the excitation of neon, argon, krypton, or xenon in a buffer of helium and argon, krypton, or xenon in a neon buffer.

EXPERIMENT

The techniques used in this study were virtually identical to those used in earlier reports [2,3]. The pulse radiolysis facility at the Argonne National Laboratory Chemistry Division Linac was used. Pulses of 30 MeV electrons of less than 40 ps duration and about 25 nC charge were used to irradiate gas samples contained in cylindrical quartz vessels with Suprasil windows. The dose per pulse was approximately 5–10 krad. Light emission was observed at right angles to the axis of the electron beam from a zone near the axis of the cylindrical cell and 2–3 cm from the window. A microchannel plate photomultiplier tube (Electro-Optical Products type FA128fQ/420) monitored the output from a monochromator.

A sampling procedure was used to obtain the emission data; electron pulse frequencies in the range 30–120 s^{-1} were used together with a 7S11 sampling unit in a Tektronix 7904 oscilloscope. The output of the sampling unit was fed—via an analog to digital converter—into an LSI-11 computer. Data files were transferred to a VAX computer for further analysis using nonlinear least-squares fitting routines.

*Permanent address: Department of Chemistry, University of Melbourne, Parkville, Victoria 3052, Australia.

Materials and procedures

Helium (Airco, "ultrahigh purity") was purified immediately prior to use by slow passage through a copper $\mathcal{U}$ tube packed with an activated molecular sieve (type 5A) maintained at liquid-nitrogen temperatures. This procedure removed traces of water, nitrogen, and oxygen from the bulk helium. The same procedure was used for neon (Matheson Research Grade). Argon (Matheson) was condensed into a storage bulb on the vacuum line and degassed several times before storage at liquid-nitrogen temperatures. Samples of up to 0.66 kPa were taken from this stored sample (equilibrium pressure at ~77 K, ~20 kPa). Krypton and xenon (Matheson Research Grade) were purified by several freeze-pump-thaw cycles. All samples were prepared on a conventional greaseless, mercury-free metal-glass vacuum line. Connections to the vacuum line were made using Cajon "ultra-torr" fittings and pressure measurements were made with an MKS Baratron (type 77) pressure gauge.

Energy deposition in irradiated gases

The range of a high-energy electron in the gas is large (meters) compared to the dimensions of the cell (~2.5 cm), so that essentially *all* the incident high-energy electrons *exit* the system. The effect of the passage of high-energy electrons is to generate secondary ionization events, but with inevitably *equal* amounts of positively and negatively charged entities. Thus, there is no excess charge in this system. It is therefore reasonable to neglect bulk space-charge effects. [This may not be the case for irradiations done with high linear energy transfer (LET) radiation such as α particles, protons, deuterons, and heavy ions.] Nevertheless, to be clear on this point, it is worthwhile to consider carefully the full action of the irradiating pulse of energetic electrons.

Dosimetry: production of charges

The charge in the incident pulse is high, ~25 nC, which is about 6×10^{10} electrons, but the beam is not "stopped" in the gas sample. The primary electron beam is largely unattenuated and passes out of the system. During its passage, it generates a spectrum of energetic secondaries. The range of the primary electrons is ~10 cm in liquid water and many meters in 1 atm of a gas such as argon. The electron beam contains a total energy of ~0.75 J per pulse, but only a small fraction (<0.1%) of this energy is transferred to the gas. This can be calculated as follows. Dosimetry measurements indicate that the absorbed energy from the beam is of the order of 10^4 rad per pulse. Since 1 rad $=6.24\times10^{13}$ eV/g, then the absorbed dose equals ~1 J/g. In a typical sample, say 0.2 atm of argon at 20°C, density$=3.33\times10^{-4}$ g/cm^3; the radiation dose adsorbed by the sample is therefore 3.33×10^{-5} J/cm^3. This is of the order of 0.04% of the incident-beam energy. Typically, when all of the secondary energetic electrons are thermalized [8], this will produce an instantaneous ion density of the order of 10^{12} cm^{-3}. The irradiation beam will thus produce a low-density plasma with charge balance.

Spatial distribution

The loss of energetic secondary electrons from the irradiation zone would result in the setting up of space-charge fields that could influence the subsequent electron-neutral interactions. The loss of a small amount of charge would produce ambipolar electric fields. Ambipolar diffusion is reported [9] to set in quickly and will reduce further electron escape rate to negligible levels over the times of observation in these studies. We believe therefore that a spatially homogeneous kinetic analysis can be used to analyze the results and that space-charge effects are not significant.

RESULTS AND DISCUSSION

The systems studied consisted of a trace amount of the rare gas—neon, argon, krypton, or xenon—in a bath gas of helium or neon. The emission from a $2p$ level of the rare gas was used to monitor the kinetics of formation and decay of that excited state. Specifically, the $2p_1$ level of neon (585 nm), the $2p_1$ level of argon (750 nm), the $2p_6$ level of krypton (762.5 nm), and the $2p_5$ level of xenon (840 nm) were used. These states were selected on the basis of greatest intensity (Ne and Ar) or accessibility (Kr and Xe). In the case of these latter gases, the majority of the $2p$ levels were outside the sensitivity range of the detector used in these studies. The kinetics of formation and decay of each of the excited states was studied as a function of the pressures of both components of the mixture. The pressure of the trace component was varied over the range 40–670 Pa at a constant helium or neon pressure of 13.3 kPa; the helium or neon pressure was varied from 6.66–66.7 kPa at a constant trace component pressure of 0.133 kPa.

A typical set of experimental data is shown in Fig. 1; the diagram shows the emission-time curve for a sample containing 0.4 kPa of argon and 13.3 kPa of helium (curve A). Background emissions (curve B) were taken for each sample at a wavelength a few nm away from the emission wavelength under observation. This enables

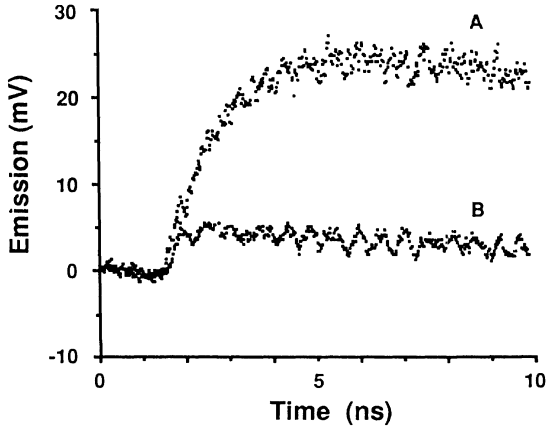

FIG. 1. Emission vs time curves for 0.4 kPa argon in 13.3 kPa helium. (A) Raw data from Ar $2p_1$ at 750 nm; (B) background at 740 nm.

Čerenkov radiation or other emissions from helium or the irradiation cell to be allowed for during analysis of the main signal.

The signal clearly grows in, reaching a maximum in 4–5 ns, then decays more slowly. Figure 2 shows this experiment conducted over a longer time scale (~50 ns), after which the signal has decayed significantly. The rise and fall of emission intensity in this way suggests a mechanism, using an Ar, He mixture as an example, of the form

$$e^-(T)+\mathrm{Ar}\xrightarrow{k_1}\mathrm{Ar}^*(2p_1)+e^- , \quad (1)$$

$$e^-(T)+\mathrm{He}\xrightarrow{k_2}\text{products} , \quad (2)$$

$$\mathrm{Ar}^*\xrightarrow{k_e}\mathrm{Ar}+h\nu , \quad (3)$$

$$\mathrm{Ar}^*+\mathrm{Ar}\xrightarrow{k_q}\text{quenched products} , \quad (4)$$

where $e^-(T)$ represents electrons with insufficient energy to electronically excite He, and reaction (2) represents the process of energy loss by elastic collision with helium. Under pseudo-first-order conditions ($[e^-(T)] \ll [\mathrm{Ar}]$ or [He]) these equations lead to the expression

$$[\mathrm{Ar}^*]_t = \frac{[e^-(T)]_0 k_1[\mathrm{Ar}]}{(k_e+k_q[\mathrm{Ar}])-(k_1[\mathrm{Ar}]+k_2[\mathrm{He}])} \times [e^{-(k_1[\mathrm{Ar}]+k_2[\mathrm{He}])t}-e^{-(k_e+k_q[\mathrm{Ar}])t}] . \quad (5)$$

(In the case of other solute gases, Ar is replaced by Ne, Kr, or Xe in helium mixtures; and in neon mixtures, the solutes are Ar, Kr, and Xe.)

If, as in systems earlier studied, the experimental emission growth-decay curves are shown to adequately fit an exponential growth-decay function, then the data can be used to determine the rate constants k_1, k_2, k_e, and k_q in the above scheme. Figure 3 shows the experimental results from Fig. 1 and fitted curve based on Eq. (5). In practice, the decay part of the data (Fig. 2) was analyzed first and was invariably found to give a good exponential fit. The decay constant thereby obtained was used as a fixed parameter in the nonlinear least-squares analysis of the data shown in Fig. 1.

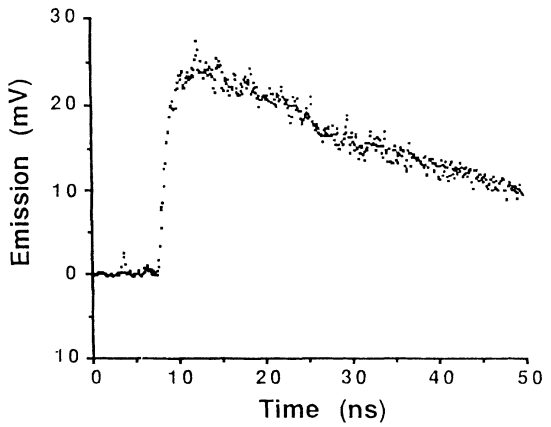

FIG. 2. Decay of Ar $2p_1$ at 750 nm for 0.4 kPa xenon in 13.3 kPa helium.

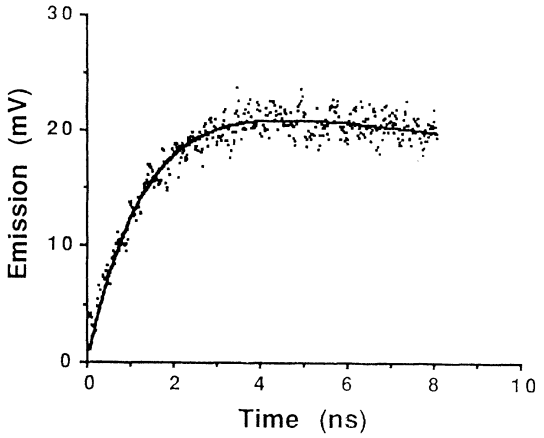

FIG. 3. Emission vs time curve from data in Fig. 1 with computer subtracted background. Solid curve: from least-squares fit to Eq. (1); dots: experimental data.

Analysis of data for a range of rare-gas and helium or neon pressures revealed the following.

(i) The formation rates were strongly dependent on the (additive) rare-gas pressure (at constant helium or neon pressure) and increased with increasing pressure of the additive (40–670 Pa).

(ii) The formation rates were significantly dependent on bulk helium or neon gas pressure (6.67–66.7 kPa).

(iii) The decay rates were weakly dependent on the helium or neon pressure and very slightly dependent on the additive rare-gas pressure.

(iv) The data for xenon in helium could not be fit well to Eq. (5).

The pseudo-first-order rate constants obtained from these analyses were found to vary linearly with pressure over the range studied. Figure 4 (line A) shows the variation of the first-order formation constant $K_1 = k_1[\mathrm{Ar}]+k_2[\mathrm{He}]$ with the argon pressure at a constant helium pressure of 13.3 kPa. The slope of this plot and similar ones for the other rare gases yields the values for k_1 shown in Table I. Data for helium pressure variation, at a constant argon pressure of 133 Pa, were similarly analyzed—Fig. 4; line B—and yielded values of k_2 in Table I. Similarly, the data for solutions of neon and krypton in helium as well as for argon, krypton, and xenon in neon, were processed to yield the results in Table I.

Xenon results

As noted above, the results for helium-xenon mixtures were fit poorly by the double exponential function, Eq. (5). The quality of the fit was especially poor at low helium pressures. Figure 5 (curve B-B) shows the fit for a mixture of 400 Pa Xe in 6.67 kPa He. The decay of this excited state was measured in a separate experiment over a longer time scale and was found to be $2.1\times10^7\ \mathrm{s}^{-1}$. This value was used as a fixed parameter in analysis using Eq. (5); the fit is clearly poor. This analytical approach

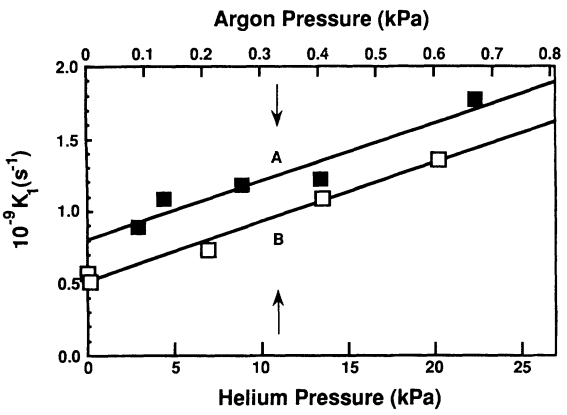

FIG. 4. (A) Black squares: variation of the formation rate constant K_1 with argon pressure at a constant helium pressure of 13.3 kPa, (B) open squares: variation of the formation rate constant K_1 with helium pressure at a constant argon pressure of 0.4 kPa.

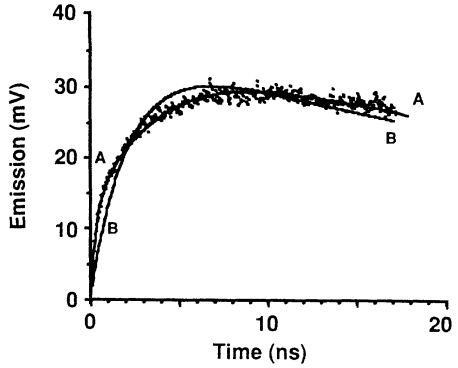

FIG. 5. Emission vs time curve from xenon $2p_5$ for a helium (6.67 kPa), xenon (0.4 kPa) mixture. Dots are experimental data; curve A-A is the fit to Eq. (9); curve B-B is the fit to Eq. (5).

shows the following features with respect to the data.

(i) Initially the data rise faster than the fitted curve.

(ii) Near to and beyond the maximum intensity, the data rise and decay more slowly than the fitted curve.

(iii) At longer times the decay is a good single exponential fit.

It is clear that more than one process is participating in the formation of this xenon excited state ($2p_5$). One characteristic of these $2p$ levels in the rare gases is the very small energy differences between some of the ten members of each $2p$ manifold *and* the ease of collisional downward deactivation. The $2p_1$ levels studied for the other gases are at the top of the manifold and have no obvious near-neighbor candidates for repopulation. The $2p_5$ level can easily be populated by collisional deactivation of the $2p_4$ level *and* maybe $2p_3$, $2p_2$, and $2p_1$. Thus an extra formation process needs to be included in the mechanism. The following is a reasonable proposal to fit this condition.

$$e^-(T)+\mathrm{Xe}\xrightarrow{k_1}\alpha\mathrm{Xe}^*+(1-\alpha)\mathrm{Xe}^{\#}\ , \tag{6}$$

$$\mathrm{Xe}^{\#}+M\xrightarrow{k_M}\mathrm{Xe}^*\ , \tag{7}$$

$$\mathrm{Xe}^*\xrightarrow{k_e}\mathrm{Xe}+h\nu\ . \tag{8}$$

In this mechanism, energetic electrons $e^-(T)$ interact with ground-state xenon to produce a fraction (α) of the excited state Xe* directly and ($1-\alpha$) of other excited states Xe# which can populate Xe* by collision with a ground-state atom M.

This mechanism can be solved analytically to give a closed form equation for [Xe*].

$$[\mathrm{Xe}^*]=K_1[e^-(T)]_0\left\{\left[\frac{\alpha}{k_e-K_1}+\frac{(1-\alpha)B}{(B-K_1)(k_e-K_1)}\right]e^{-K_1t}-\frac{(1-\alpha)B}{(B-K_1)(k_e-B)}e^{-Bt}\right.$$
$$\left.-\left[\frac{\alpha}{k_e-K_1}+\frac{(1-\alpha)B}{(B-K_1)(k_e-K_1)}-\frac{(1-\alpha)B}{(B-K_1)(k_e-B)}\right]e^{-k_et}\right\}\ , \tag{9}$$

TABLE I. Experimental values of k_1 and k_2.

	$k_1(10^{-9}$ cm^{3}s$^{-1})$ Buffer gas			$k_2(10^{-9}$ cm^{3}s$^{-1})$ Buffer gas rate constant	
Solute	None[a]	Helium	Neon	Helium	Neon
Neon	3.5	9.5±1.0		0.20±0.02	
Argon	9.5	5.8±0.7	5.5±0.4[b]	0.17±0.03	
			4.2±0.4[c]		
Krypton	8.0	8.3±1.1	8.6±0.8	0.18±0.030	0.058±0.015
Xenon	11.5	35±6	12±1	0.035±0.006	0.02±0.01

[a]For comparison, the values of k_1 obtained in the pure rare gases [3] are given in this column.
[b]Obtained by observing emission from the $2p_1$ level of argon at 771 nm.
[c]Obtained by observing emission from the $2p_3$ level of argon at 858 nm.

where $B=k_M[M]$, and $K_1=k_1[\mathrm{Xe}]$, or more correctly, $K_1=k_1[\mathrm{Xe}]+k_2[M]$. This will allow for $e^-(T)+M\xrightarrow{k2}$ products, which cannot excite Xe. Also, k_e is the decay constant for Xe* (more correctly, this term will be $k_e'+k_q[M]$ where k_q is a quenching constant for He and/or Xe interacting with Xe*, and k_e' is the true radiative lifetime), and $[e^-(T)]_0$ is the initial concentration of energetic electrons.

The mechanism presents certain restrictions to the valid nonlinear least-squares fit to Eq. (9).

(i) For a given subexcitation electron distribution, α should be independent of xenon or helium pressures.

(ii) To be consistent with data for the other systems, K_1 should show a linear dependence on xenon pressure and give a value for $k_1>2\times10^{-9}$ cm^3 s^{-1}.

(iii) At constant xenon pressure, B should be a linear function of helium pressure and give a value of k_M similar to that expected for the quenching of these excited states, i.e., 10^{-11}–10^{-10} cm^3 s^{-1}.

The data for helium-xenon mixtures were fitted to Eq. (9) with a four parameter fit, i.e., K_1, B, k_e, and α. The following procedures were carried out and observations were made.

(i) For the helium-xenon systems, 13.3 kPa He and 67–670 Pa Xe, all variables were allowed to float. It was noticed that α ranged from 0.30–0.45; K_1 was $\sim10^9$ s^{-1} and B was $\sim10^8$ s^{-1}.

(ii) If the decay of Xe*, measured in separate experiments on longer time scales (as in the other systems), was used to fix the parameter k_e, then α varied only from 0.36–0.41. The average over a series of analyses was 0.38 ± 0.02.

(iii) If $\alpha=0.38$ and k_e (experimental value $\sim2\times10^7$ s^{-1}) were used as fixed parameters, then a good fit, such as is shown in Fig. 5 (curve A-A), was obtained. For each system analyzed, the value of k_e observed for the specific system was used.

The results show the predicted linear dependence of K_1 on Xe (Fig. 6) and B on He pressure (Fig. 7). From these

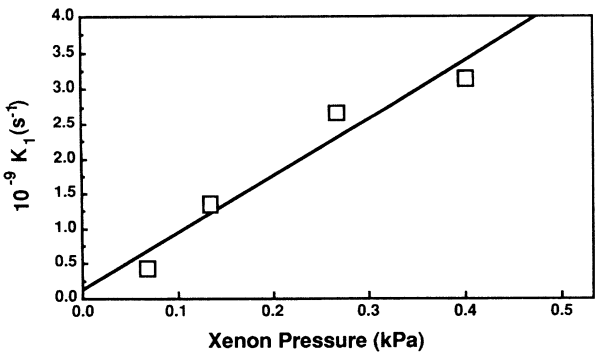

FIG. 6. Variation of K_1 [from Eq. (9)] with xenon pressure at 13.3 kPa helium.

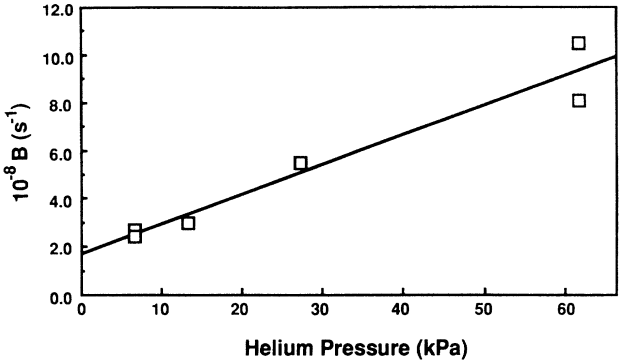

FIG. 7. Variation of B [from Eq. (9)] with helium pressure at 0.4 kPa xenon.

plots, values for the rate constants were determined as $k_1=3.5\pm0.8\times10^{-8}$ cm^3 s^{-1}, $k_M=4.1\pm0.5\times10^{-11}$ cm^3 s^{-1} (for He), $k_2=3.5\pm1.3\times10^{-11}$ cm^3 s^{-1} (determined from the intercept of Fig. 6).

$B(k_M)$ was not discernibly affected by variation of the xenon pressure in the range 67–400 Pa, in the presence of 13.3 kPa of helium. Conversion of Xe# to Xe* must be predominantly by collisions with helium.

The values of k_1 and k_2 are included in Table I and are directly comparable with the values for the other systems. The value for k_M, the rate constant for the quenching of Xe# by helium, of $4.1\pm0.5\times10^{-11}$ cm^3 s^{-1} is reasonable when compared with the value 6.45×10^{-11} cm^3 s^{-1} observed earlier [3] for the quenching of *this* particular excited state by xenon itself.

Excited state quenching rates

From the analysis of the growth-decay curves over the longer times scales (50 ns), the decay of the excited state could be monitored. The curves showed good first-order decays at long times and increased in decay rate with increase in pressure. From this data, the quenching of the excited state of the trace additive by the bulk rare gas could be determined. In some cases, it was possible to determine the quenching by the trace gas itself. The data for these various mixed systems are summarized in Table II. Generally speaking, the quenching rate constants for the various $2p$ levels in these rare gases are all in the range $10^{-12}-8\times10^{-11}$ cm^3 s^{-1}. This range is typical [10] of the rate constants expected for collisional quenching of rare-gas electronic excited states.

CONCLUSIONS

Direct observations show that the formation of electronic excited states in pulsed electron irradiated gaseous systems is delayed well beyond the temporal limits of the excitation pulse. The rate of formation is pressure dependent indicating some form of two-body collisional process. Analysis of intensity vs time curves by conventional kinetic procedures gives the results in Table I, which show that the formation rate constant for the electronic excited states increases with increasing atomic weight of

TABLE II. Experimental excited-state quenching rate constants.

Buffer gas	k_q, buffer (10^{-11} cm^3 s^{-1})	Solute gas	k_q, solute (10^{-11} cm^3 s^{-1})
He	5.3±0.4	Ne	not detectable
He	0.45±0.10	Ar	not detectable
He	1.5±0.5	Kr	not detectable
He	0.17±0.08	Xe	10±4
Ne	0.25±0.10	Kr	11±1
Ne	0.64±0.04	Xe	9.9±4.5

the additive rare gas. There appears to be no significant difference between helium and neon as a buffer gas.

Using the subexcitation electron model, the rate constant would depend upon the superposition of the subexcitation electron spectrum [11] and the cross section versus energy function for the rare-gas excited state. The subexcitation electron spectrum above about 10 eV only shallowly decreases with energy in a structureless distribution. This goes up to about 20 eV in helium and about 17 eV in neon. Secondary electrons above these energies lose energy very rapidly by inelastic processes to the bulk gas, and their lifetime is very short—of the order of 10^{-11} s—compared to the observed formation times of up to 20 ns recorded in these experiments.

The cross section for production of the excited state of the additive rare gas over the energy range from its threshold to the limit of the subexcitation domain will vary significantly. In the case of a helium-neon mixture, the only active electron energy range is from the subexcitation limit of helium (19.8 eV) to the energy threshold of the neon excited state ($2p_1$) at 18.96 eV. The cross section for excitation will be changing rapidly over this very narrow energy range—less than a volt—since the electron energy is close to the threshold value. In the case of the other mixtures with helium, the energy window between subexcitation and the threshold of the emitting state is wider; for argon $2p_1$, the threshold is 13.2 eV and the window is 6.6 eV; for krypton $2p_6$, the threshold is 11.3 eV and the window is 8.6 eV; for xenon $2p_5$ the threshold is 10.1 eV and the window is 9.7 eV. The window gets wider with increasing atomic weight of the rare-gas additive. Similarly, with neon as a bulk gas, the subexcitation electron energy ranges can be obtained from the subexcitation limit of 16.6 eV. Using the thresholds given above, one obtains energy windows of 3.4 eV for argon $2p_1$, 5.4 eV for krypton $2p_6$, and 6.5 eV for xenon $2p_5$.

In our experiment, the energy distribution of subexcitation electrons changes during the time scale of the experiment. The initial Platzman-like distribution [5,11] produced in the bulk gas subsequently evolves through the subexcitation range to and through the inelastic excitation range of the additive. Eventually, a Maxwellian distribution is attained as the electron distribution approaches thermal energies.

In other words, the mean energy of the secondary swarm changes with time. Thus we should see a variation of the rate constant over the duration of the experiment in line with the expected variation of the cross section of the excitation with electron energy. The temporal data that we analyzed do not show any marked deviation from a single exponential with time, although the noise on the signals could cover such an effect if it is relatively small.

Therefore, the conclusion we draw is that the combination of the effects of mean electron energy changes on both the excitation coefficients and the parallel momentum-transfer processes do not cause a marked time dependence of the rate constant for formation of these excited states. This implies that the modeling of the time-dependent decay of energetic electrons in simple gas mixtures can be approximated by relatively simple kinetic laws. This is, in part, reasonable in light of the known featureless structure of the subexcitation electron distribution.

Table I (column labeled "none") shows previously reported results for pure rare gases where a similar delayed production of emission was observed [3]. In this case, secondary electrons are responsible for the delayed excited-state production but, by definition, they cannot be called subexcitation electrons. These results for the pure gases are not markedly different from those in the mixed systems, which indicates the similarity of the behavior of secondary electrons in the pure rare gases and subexcitation electrons in the mixed systems.

In the case of argon in excess neon, two argon $2p$ levels were monitored. There was no difference, within experimental error, in the formation constants for the two excited levels of argon. This is consistent with a common precursor mechanism—subexcitation electrons—for the formation of these states.

If this mechanism is correct, then the rate constant k_2, for the energy loss of electrons by elastic processes involving helium in the presence of traces of neon can be estimated from known cross-section data. Essentially, the electron needs to lose energy sufficient to cross the window from 19.8–18.96 eV (the latter being the energy threshold of the $2p_1$ state of neon) before it loses energy to neon by inelastic processes. The number of collisions needed is the size of this energy gap divided by the energy loss per collision, i.e., $\Delta E/dE_{\text{coll}} = (19.8-18.96)/dE_{\text{coll}}$. Assuming the average energy of the window is $E = 19.4$ eV, $dE_{\text{coll}} = 2m_e E/M_{\text{He}}$ (where m_e is the electron mass and M_{He} is the mass of helium), or 5.319×10^{-3} eV per collision. For the 0.84-eV window, the number of collisions n_{coll} is 158. From Hayashi [15] we use an average momentum-transfer cross section σ_{mt}, over this window of 3×10^{-16} cm^2, and taking the effective rate constant for disappearance of the subexcitation electron due to

elastic collisions with the buffer gas as $\sigma_{mt} \times v_e / n_{coll}$ (where v_e is the average velocity of the electron for the window), we obtain 5.0×10^{-10} cm^2 s^{-1}. This value is high compared with the experimental result of 2.0×10^{-10} cm^{-2} s^{-1} given in Table I. A similar calculation for neon gives 4.3×10^{-11} cm^{-2} s^{-1} compared with the experimental value of $5.8 \pm 1.5 \times 10^{-11}$ cm^{-2} s^{-1}. The agreement is sufficiently good to give confidence in both the experimental determination and the kinetic analysis of these time-dependent processes. A similar analysis of the formation rate constant k_1, is not valid since for the solute gas both elastic and inelastic processes are active in the energy window between the lowest excitation threshold of the bulk gas and the threshold of the observed excited state.

We conclude, therefore, that the delayed formation of electronic excited states in dilute binary rare-gas mixtures is directly attributable to the degradation of subexcitation electrons generated from the bulk gas. A similar pattern of delayed formation of emission was observed in diatomic (N_2) [1] and polyatomic (hydrocarbon) systems [2]. The phenomenon displays a strong dependence on the pressure of the probe and a weaker one on the bulk gas pressure. This mechanism associated with these observations has been identified unequivocally [12] as the inelastic and elastic scattering of subexcitation electrons. The results show that the derived rate constant for energy loss to the buffer gas is about three times less for neon than for helium. This is in keeping with the poorer thermalization behavior of neon compared to helium and compares well with observations in nitrogen mixtures with these gases [1].

Some cross-section data are available [13,15] for elastic collisions and inelastic processes in these monatomic gases. It should thus be possible to perform calculations similar to those done by Naleway [7] and, more recently, by Dillon, Inokuti, and Kimura [14] to accurately model the time decay of a subexcitation electron swarm in these mixed gases. Such calculations are under way and will be reported in a later communication.

ACKNOWLEDGMENTS

R. Cooper would like to acknowledge support from the Australian Research Council (ARC) and the Radiation and Photochemistry Group at Argonne National Laboratory. The authors would like to thank M. Inokuti and M. Dillon for helpful discussions, and D. Ficht, G. Cox, and E. Kemereit for operating the linac. The invaluable discussions with J. Warman (T.U. Delft) and R. Morrow (CSIRO) are gratefully acknowledged. This work was performed under the auspices of the Office of Basic Energy Sciences, Division of Chemical Science, US-DOE under Contract No. W-31-109-ENG-38.

[1] R. Cooper, L. S. Denison, and M. C. Sauer, Jr., J. Phys. Chem. **86**, 5093 (1982).
[2] L. S. Denison, R. Cooper, and M. C. Sauer, Jr., J. Phys. Chem. **90**, 683 (1986).
[3] R. Cooper and M. C. Sauer, Jr., J. Phys. Chem. **93**, 1881 (1989).
[4] R. L. Platzman, *Symposium on Radiobiology, Oberlin College, 1950,* edited by J. J. Nickson (Wiley, New York, 1952), pp. 97–116 and pp. 139–176.
[5] R. L. Platzman, Radiat. Res. **2**, 1 (1955).
[6] M. Inokuti, in *Molecular Processes in Space,* edited by T. Watanabe, I. Shimamura, M. Shimizu, and Y. Itikawa (Plenum, London, 1990), pp. 65–86.
[7] C. Naleway, M. Inokuti, M. C. Sauer, Jr., and R. Cooper, J. Phys. Chem. **90**, 6154 (1986).
[8] J. M. Warman and M. C. Sauer, Jr., J. Chem. Phys. **62**, 1971 (1975).
[9] W. P. Allis and D. J. Rose, Phys. Rev. **93**, 84 (1954).
[10] See, for example, G. Inoue, J. K. Ku, and D. W. Setser, J. Chem. Phys. **81**, 5760 (1984).
[11] D. A. Douthat, Radiat. Res. **61**, 1 (1975).
[12] M. Inokuti, *Radiation Research,* Proceedings of the 8th International Congress of Radiation Research, Vol. 2, Edinburgh, 1987, edited by E. M. Fielden, J. F. Fowler, J. H. Hendry, and D. Scott (Taylor and Francis, London, 1987), pp. 250–254.
[13] E. Eggarter, J. Chem. Phys. **62**, 833 (1975).
[14] M. A. Dillon, M. Inokuti, and M. Kimura, Radiat. Phys. Chem. **32**, 43 (1988).
[15] M. Hayashi, in *Gaseous Electronics and Its Applications,* edited by R. Crompton, M. Hayashi, D. E. Boyd, and T. Makabe (Kluwer Academic, Boston, 1991), pp. 9–83.